Submillimeter T2 weighted BOLD fMRI of human visual cortex

Chapter 5

Summary and discussion

MRI acquisitions present an abundance of trade-offs and compromises between competing factors for optimal results, and fMRI techniques constitute no exception to this rule. The choice of the optimal functional contrast mechanism (T_2^* weighted BOLD, T_2 weighted BOLD, CBV, CBF) for a given application is fundamental and by no means trivial (but often dictated by practical considerations). After opting for a basic experimental design and imaging sequence type, the imaging parameters need to be set to satisfy the needs of a given application (e.g. high spatial resolution mapping, encoding/decoding of brain states, whole-brain resting state) for subject safety (SAR and peripheral nerve stimulation limits), spatial resolution, temporal resolution, spatial coverage, distortions, short experiment duration, functional specificity, and functional sensitivity all at the same time (see Figure 5-1). All current high resolution fMRI approaches have their pros and cons, and the fact that a remedy for a typical downside of a given approach in special cases might be at hand makes things only more confusing. The methodological contributions of this thesis extend the knowledge in the field of T_2 weighted ultra-high field fMRI, exploring possibilities and limitations of the acquisition and analysis techniques for this contrast mechanism. In this chapter, we will summarize our empirical findings and then explore two aspects of particular relevance to high resolution fMRI further: Avoidance of macrovascular signals and precise co-registration with anatomical reference images. Finally, we will give an account of personally presumed future developments and open challenges.

Summary

In Chapter 2 we have shown how two T_2 weighted fMRI sequences, 3D-GRASE and 2D SE-EPI compare at 7 T in a submillimeter resolution experiment. 3D-GRASE yielded superior specificity and sensitivity over SE-EPI with large field of view. Spatial coverage and image blurring were better in SE-EPI. The superior sensitivity was reflected in more robust activations in a visual task. Besides the SNR-beneficial 3D acquisition in 3D-GRASE, the 2D multi-slice slice profiles were identified to hamper the tSNR in 2D SE-EPI. In high resolution cortical depth profiles, 2D SE-EPI revealed an increase of BOLD signal changes towards superficial layers, resembling previously observed GE-EPI profiles but with a smaller slope. The fact that in deep cortical gray matter the signal changes were similar suggested that principally, similar contrast mechanisms were at work, however, the

increase towards the surface was in line with a higher T_2^* contrast contamination in 2D SE-EPI. Moreover, we demonstrated that the difference in superficial layers was not a mere consequence of blurring by an analysis of smoothed 2D SE-EPI data and of the angle between the cortex normal and the 3D-GRASE slabs in two orthogonal orientations. We concluded that 3D-GRASE is the preferred method for the investigation of fine functional structures, however acknowledging the limited spatial coverage and strong slice blurring.

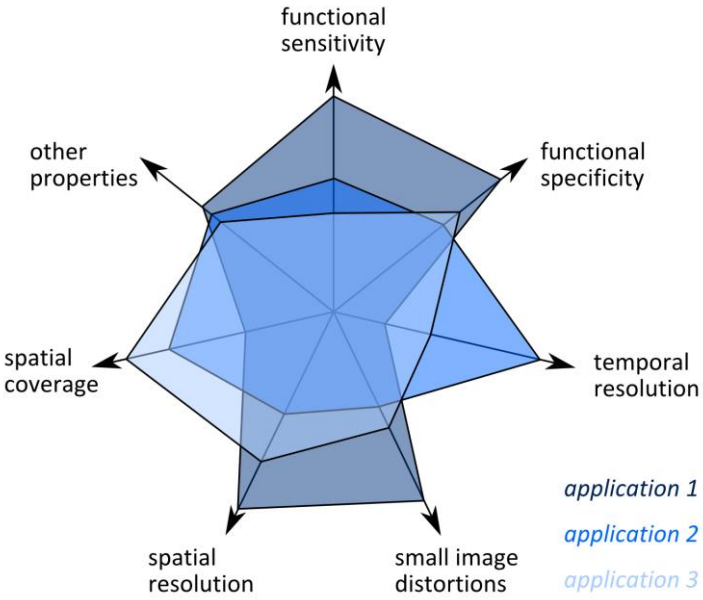

Figure 5-1: Example profiles of required characteristics of fMRI applications. Multiple properties (dimensions) are displayed in a polar diagram.

In Chapter 3, we addressed these issues of 3D-GRASE by introducing a variable flip angle refocusing approach for 3D-GRASE based on extended phase graph theory. This made a simultaneous improvement of coverage and image blurring possible. The VFA approach grants more flexibility in the use of 3D-GRASE to find balance points of the acquisition properties mentioned above which suit the application best. Specifically, coverage and image blurring could be significantly improved compared to the standard

180° refocusing approach at little cost in functional sensitivity. Moreover, SAR becomes significantly less of a limitation using the smaller refocusing angles. Despite the fact that tSNR was reduced in the VFA approach, functional sensitivity was partly maintained due to a small observed increase in functional contrast in the functional experiment at 7 T. This is mediated by a shift of signal towards the longer TE pathways in stimulated echo pathways. The agreement of simulations and experimental data was first validated in phantom measurements. In-vivo, we were able to obtain blurring similar to that observed in 2D SE-EPI in chapter 1. The VFA approach was more susceptible to B_1^+ inhomogeneity yielding reduced tSNR and functional sensitivity when the transmission was insufficient.

In Chapter 4, we explored the possibilities of human anatomical and functional MRI at 9.4 T further. With a specialized RF coil with spatially limited transmit- and receive profiles, we were able to conduct the experiments well within the SAR limits using a non-subject-specific B_1 shim with high RF efficiency and sufficient homogeneity. Good anatomical contrast was observed in T_1 weighted MPRAGE acquisitions adapted to the relaxation times at 9.4 T. Further, high resolution (0.35 mm isotropic) T_2^* weighted data yielded sufficient information to observe clear differences in cortical depth dependent profiles between visual areas V1 and V2 associated with the co-localization of iron with myelin in the Stria of Gennari. A routine population receptive field experiment yielded excellent results affirming the expected SNR advantage of ultra-high field beyond 7 T. By the means of the VFA approach, we were able to apply 3D-GRASE also at 9.4 T for a functional mapping experiment at 0.7 mm isotropic nominal resolution. These measurements showed significant differences in ocular dominance between retinotopically defined V1 and V2. Further, our preliminary results revealed a patchy organization of ocular dominance in V1 of one of the two volunteers. This organization was found to be consistent across cortical depth.

Avoiding macrovascular signals in T_2^* and T_2 weighted BOLD data

Functional specificity is the key advantage of high field T_2 weighted BOLD over T_2^* weighted BOLD fMRI, which has previously been demonstrated extensively (in methodological and application studies, see Introduction for details). However, in most imaging aspects aside of functional specificity, GE-EPI sets high standards, particularly functional sensitivity. Could it be

that the overall higher sensitivity over-compensates the lower specificity, or is the higher specificity of T_2 more beneficial? A few aspects of this question will be outlined in the following section.

To begin with, taking a purely quantitative stand-point, it must be noted that the expected signal changes from micro-vasculature are not fundamentally different between T_2 and T_2^* weighted BOLD imaging. For both, extravascular signal changes are simulated to be between 1 and 2 % at ultra-high field (Uludag et al., 2009). The intravascular component is negligible. Empirically, Yacoub et al. (2005) reported the T_2^* signal to be on average 1.3 ± 0.1 times higher than the T_2 signal in gray matter at high spatial resolution at 7 T. Stronger differences in sensitivity must be the result of lower tSNR, and in fact, lower tSNR is reported in comparative studies when different TEs and relaxation times are taken into consideration (Harmer et al., 2012; Boyacioglu et al., 2014). This reduction in tSNR in T_2 weighted data could be a consequence of poor slice profiles and saturation effects, as discussed in Chapter 2 of this thesis. The spin-echo signal suffers more strongly from imperfect slice profiles because of the combined $\sin(\pi \cdot f/2)^3$-dependence on the RF scaling factor f of excitation and refocusing pulse, as compared to $\sin(\alpha_E \cdot f)$ in gradient-echo, where α_E is the Ernst angle. Technical imperfections could thus explain a significant part of the difference in sensitivity - irrespective of potential differences in physiological noise contributions. The discrepancy of results between Yacoub et al. (2005) and Triantafyllou et al. (2009) with regard to physiological noise in T_2 weighted data is however noted: While the former reported a constant ratio of physiological to thermal noise with increasing voxel size, the latter reported a similar increase as in T_2^* weighted data. Panchuelo et al. (2015) used retinotopic response patterns to demonstrate that the CNRs of T_2 and T_2^* weighted BOLD imaging converge when the cortical distance between neighboring responses is reduced to 1 mm. Unfortunately, the study did not investigate smaller distances, which would reveal whether T_2 weighted BOLD excels at higher resolution.

One argument for the utility of a sensitive but unspecific approach is that non-specific signals should cancel each other out in a differential fMRI approach. However, this is only true for balanced conditions, in which the unspecific signals are zero-mean (Polimeni et al., 2010). Further, unrelated signal changes impede the quality of activation estimates (e.g. predictors in a GLM are less efficient). As a remedy, it has been suggested to mask image

positions which are known to contain large vessels, particularly large pial vessels (Barth and Norris, 2007; Koopmans et al., 2010) in T_2^* weighted data, or, in a more drastic form to ignore all data except from middle cortical depth altogether (Goncalves et al., 2015). This approach exploits that large vessels appear dark and tend to have high dynamic signal changes (Olman et al., 2007), or the position of large vessels is obtained from other, co-registered scans. This approach is viable under two conditions: 1) The spatial resolution is sufficiently high to rule out partial volume effects from surface vessels in middle layers (and below). 2) It can be afforded to discard the tissue affected by the vessels, which may be near or far away. This can be the case, e.g. when the aim of the study is to find evidence for the presence of information in a given region or cortical layer using multi-variate pattern analysis (Haxby et al., 2001; Smith and Muckli, 2010; Muckli et al., 2015), or when data can be averaged across a larger cortical region of interest. However, if the intention is to *map* a given region, the approach does not present a solution. In particular, ignoring signals from superficial layers preempts the possibility to draw any conclusions about columnar (that is vertical, depth-dependent) organization or to target feedback connections which terminate in superficial layers (Muckli et al., 2015). At best, the knowledge about the presence of macrovasculature may give a good estimate of the reliability of the functional data at a given location, as has also been demonstrated at lower resolution (Winawer et al., 2010). Nonetheless, Muckli et al. (2015) were able to decode, which partly occluded visual scene subjects viewed, from superficial cortical layers using GE-EPI in a retinotopic quadrant, which did not receive any visual input. The decoding accuracy was improved after removing non-specific venous signals. T_2 weighted 3D-GRASE measurements in the same subjects yielded lower decoding accuracies. This underscores the potential of T_2^* weighted BOLD for *decoding* applications, even in superficial layers.

Recent experiments (Moerel et al., under review) show that at high resolution the fidelity of gray matter voxels is inversely correlated with the distance to the nearest (medium-sized to large) blood vessel (both tangentially or radially to the cortex) as detected by a time of flight angiography. This is also in line with the observation that physiological noise affects superficial cortical layers stronger than deeper layers (Polimeni et al., 2015) and the concomitantly reduced spatial specificity in

superficial layers (Polimeni et al., 2010). To what extent responses in middle and deep layers are affected by pial vein reactions is not clear yet. When critically assessing the successful early reports of ODCs and orientation columns using thick tangential slices (Menon et al., 1997; Cheng et al., 2001; Yacoub et al., 2007; Yacoub et al., 2008) it must be stated that the columnarity was informed from knowledge from invasive animal research and post-mortem human data. Which cortical depths (or laminae) contributed to the collapsed maps is unknown, and without the similarity to primate cortical organization, strictly speaking one could only draw the very limited conclusion that tuning e.g. for ocular preference is not opposite at different cortical depths and hence does not cancel out. Importantly, such inference from animal literature is not given for higher cognitive function, where the non-invasiveness of fMRI truly unfolds its power. Whether sampling only deep layers using GE-EPI would yield spatial maps more similar to those obtained using more specific SE-EPI is unknown, however, experimental findings showed that the specificity of GE-EPI is slightly lower than that of 3D-GRASE at deep and middle cortical depth, and biases may be introduced in GE-EPI independent of cortical depth (De Martino et al., 2013). This may be either due to long-range effects of large pial vessels, or due to the contribution of intracortical veins, which drain a territory of several square millimeters in deep layers (types V4 and V5), and even transport venous blood from the white matter underneath (type V5) across the cortex (Duvernoy et al., 1981).

A relevant controversy for this context was initiated when it was shown that the orientation of visually presented grating stimuli could be decoded from responses in early visual cortex using multivariate pattern analysis (Kamitani and Tong, 2005), although orientation columns are much smaller than the used low imaging resolution in the GE-EPI experiment. The hypothesis was that the origin of the differential signals were slight sampling biases of orientation columns, but it was countered by showing that a broad-scaled organization could explain the high decoding accuracy (Freeman et al., 2011). Similarly, at higher resolution, GE-EPI might provide enough overall sensitivity to provide *information* about the brain state, however, resulting spatial maps must be treated very carefully because of the functional point-spread. This was demonstrated by Shmuel et al. (2010) reanalyzing the GE-EPI ODC data from Yacoub et al. (2007). Test-retest stability is an important indicator for the reliability of obtained maps.

Mixed results with GE-EPI might point at insufficient functional resolution for the investigated structure (Yacoub et al., 2007). As a consequence, more recent studies investigating fine-grained structures (Zimmermann et al., 2011; Goncalves et al., 2015) have adapted a modeling approach similar to as by Chaimow et al. (2011) to examine the possibility of picking up biases rather than real topographic representations of unknown spatial scale. In this modelling approach, a putative columnar organization of various sizes and other properties is modelled, and the effects of BOLD point-spread and image sampling are considered.

Finally, the question has to be addressed carefully to what extent larger vessels go unnoticed and are included in the analysis. Draining venules in the cortex have a diameter of 20 to 150 µm (Duvernoy et al., 1981; Polimeni et al., 2010). In this regime, there are already distinct differences in the sensitivity of T_2 and T_2^* weighted BOLD due to the static broadening effect (Uludag et al., 2005), however, despite the signal reduction also surrounding the vessel in T_2^* weighted imaging, these may not be seen even at high spatial resolution fMRI. Hence, fine-grained laminar functional organization might still be clouded by the non-differential response stemming from these. Finally, the notion that cortical vascularization is at least linked to the functional architecture which it supports, has been proposed (Gardner, 2010). If future research proves this hypothesis right to a finer scale than currently known (Harrison et al., 2002), researchers may worry a little less about sensitivity to medium sized blood vessels in the cortex.

Co-registration with structural images

The study reported in Chapter 4 pushes the spatial resolution both in functional and anatomical acquisitions. In this high resolution domain, the co-registration with structural images with strong anatomical contrast, particularly WM/GM contrast has proven useful, but distortions of high spatial resolution functional data impose difficulties. The reduced distortions of short EPI trains as in zoomed 3D-GRASE have been mentioned at the appropriate places in the previous chapters. However, when larger areas require a precise alignment, the residual distortions will again impede the analysis. Sequences which are virtually free of distortions may present a solution. Promising candidates, which also provide a contrast similar to T_2 weighting have recently been presented (Auerbach et

al., 2002; Ehses et al., 2013; Goa et al., 2013; Hua et al., 2013b; Goa et al., 2014; Scheffler and Ehses, 2015). It should, however, be noted that even these sequences have distortions because of gradient nonlinearities and susceptibility induced B_0 inhomogeneity. When they are acquired with a different slice prescription than the reference images, residual distortions still hamper the alignment. Moreover, the structural reference scans are also slightly distorted (although the PSF has been improved by the application of variable flip angle echo trains and improved acquisition order (Mugler et al., 1992; Deichmann et al., 2000; Stöcker and Shah, 2006) and accelerated imaging (Van der Kouwe et al., 2014)). Nonetheless, the co-registration might not fulfill the strict requirements of high-resolution fMRI so that segmentation on the basis of the functional data itself (e.g. averaged across time for better SNR) may be the only alternative. This is possible when the functional data has sufficient anatomical contrast. If this is not the case, the closest proxy to this is an anatomical acquisition with the same distortions and same slice prescription. This approach has recently been revived for T_1 weighted inversion recovery EPI data (Clare and Jezzard, 2001; Renvall et al., 2014), and may hold great potential for high resolution fMRI.

Challenges and future directions

The number of research centers operating high field MRI scanners has increased steadily in recent years. Soon, commercial 7 T systems with clinical CE and FDA approval will be on the market. The growing user group will hopefully nourish further methodological advances in the field of high resolution fMRI and enable exciting applications in the human brain. Experimental set-ups are exploring double digit field strengths (10.5 T operational at CMRR, Minnesota), and chances are that technical developments necessitated by higher field also translate to improved imaging at lower field strength, as it was the case between 7 T and 3 T. Time and again, innovations have revolutionized the way MRI is performed – compressed sensing (Lustig et al., 2007) and MR fingerprinting (Ma et al., 2013) to name just two recent examples. If one ventures a prediction, one can only start out from the currently conceivable techniques. In the following, we will therefore try to identify areas of development in the domain of high resolution fMRI acquisition.

Image acquisition and reconstruction

The importance of the imaging PSF has been stressed in this thesis. The blurring effect of signal decay throughout an echo train in EPI, 3D-GRASE, or TSE has been well characterized in the literature, but an additional blurring effect occurs from inconsistencies of the phase along the direction in question. Characterizing and correcting such phase inconsistencies caused by subject motion or other physiological contributions would further improve the PSF of 3D-GRASE. fMRI sequences with better point spread have been mentioned in the above section. They are promising for precise measurements; however, for serious application in submillimeter resolution fMRI, sufficiently high functional sensitivity remains to be demonstrated as of now. The lower temporal efficiency than in echo-train sequences impedes their sensitivity and typically requires moderately high acceleration factors for acceptable temporal resolution (Hua et al., 2013b; Scheffler and Ehses, 2015). Application of reduced field of view imaging to T2prep-GRE or SSFP approaches might overcome these hindrances.

Such reduced field of view techniques can be realized using parallel transmission (pTX) (Katscher et al., 2003; Zhu, 2004), which will see wider application in high field fMRI, especially in T_2 weighted BOLD imaging. Zoomed imaging approaches can benefit from pTX, whether in the form of more efficient outer-volume suppression or of 2D or even 3D spatially selective pulses. Tightly linked to improved RF coil designs, pTX has great potential to improve the image acquisition because of the crucial dependence on the precision of RF pulses in spin-echo sequences (particularly echo-train sequences such as 3D-GRASE), and the currently limiting factor of power deposition (SAR). PTX pulse design can accommodate both aspects (Wu et al., 2013). This way, SNR and spatial coverage in multi-slice imaging will be improved. Further, pTX will improve simultaneous multi-slice acquisitions (Poser et al., 2014), which have undergone substantial developments themselves to set new standards in imaging speed (Setsompop et al., 2013; Ugurbil et al., 2013; Xu et al., 2013).

Concomitantly, the supervision of safe operation with regard to power deposition and tissue heating is in need of future improvement at two levels. Fundamentally, possible divergence of SAR and tissue heating currently require additional safety margins (Shrivastava et al., 2008 and

references therein). Improvements in this aspect would be highly desirable, e.g. direct, precise, and accurate temperature measurements. However, given the slow pace in this domain thus far, this may not be within reach soon. Practically, the current supervision by virtual observation points (Eichfelder and Gebhardt, 2011) slows down the system operation hindering the effective use of multiple different pTX pulses altogether, and improved computations would facilitate the application.

Comparison of different acquisition approaches

Competing characteristics of the image acquisition such as spatial coverage, functional specificity, and functional sensitivity have been mentioned in the beginning of this discussion. In the multi-dimensional space spanned by these characteristics, different applications require very different profiles (see Figure 5-1). Methodological improvements help to extent the accessible volume in this space. Ideally, one axis, e.g. spatial resolution, could be extended thanks to an innovation without compromising another one, but realistically, most if not all novel approaches have their drawbacks (at least in the moment of their introduction). Over time, a large diversity of different functional contrasts and acquisition methods has developed and to this end, no overall optimal strategy for all high resolution fMRI studies in humans has been found. 2D GE-EPI is the de facto standard, and comparisons between divergent "branches" of methods are scarce. More comparisons would be desirable to obtain a more coherent, informed picture of the pros and cons of different approaches. Research collaborations between centers to fuse the expertise in the various approaches seem to be a necessary requirement for the successful and neutral assessment of different techniques. Establishment of a reference experiment with a known "gold standard" would be desirable. Such a gold standard would have to be based on well-known examples of neuronal activity.

The assessment of different approaches should go hand in hand with an advance in theoretical modeling at multiple levels. To this end, many experimental design choices are still led by intuition rather than solid simulations. For example, when intending to map a columnar structure, to what extend are partial Fourier and/or accelerated imaging acquisitions beneficial given the difference in SNR, distortions, and image blurring? Given the profile of BOLD activations in k-space (which differs from that of

static images), is tSNR the optimal target property to be maximized or could the acquisition be tailored to capture BOLD patterns best? Can the slightly higher sensitivity to capillaries of GE-EPI afford its lower specificity compared to T_2 weighted BOLD, or should researchers invest more time in techniques with even lower sensitivity and higher specificity such as perfusion or CBV based contrasts? Given the spatio-*temporal* BOLD PSF, would joint changes in stimulus presentation and data acquisition produce better results? It is evident that the answers to such questions differ depending on the specific application, e.g. mapping versus decoding. However, answers could only be found in synergy of simulations and empirical studies such that eventually, critical balance point values of diverse imaging characteristics might be found.

References

Auerbach, E.J., Heberlein, K., and Hu, X. (2002). High-resolution T2 fMRI at high magnetic fields using PSIF. *Proceedings of the 10th Annual Meeting of ISMRM, Honolulu, Hawaii*, 2345.

Barth, M., and Norris, D.G. (2007). Very high-resolution three-dimensional functional MRI of the human visual cortex with elimination of large venous vessels. *NMR Biomed* 20, 477-484. doi: 10.1002/nbm.1158.

Boyacioglu, R., Schulz, J., Muller, N.C., Koopmans, P.J., Barth, M., and Norris, D.G. (2014). Whole brain, high resolution multiband spin-echo EPI fMRI at 7T: A comparison with gradient-echo EPI using a color-word Stroop task. *Neuroimage* 97, 142-150. doi: 10.1016/j.neuroimage.2014.04.011.

Chaimow, D., Yacoub, E., Ugurbil, K., and Shmuel, A. (2011). Modeling and analysis of mechanisms underlying fMRI-based decoding of information conveyed in cortical columns. *Neuroimage* 56, 627-642. doi: 10.1016/j.neuroimage.2010.09.037.

Cheng, K., Waggoner, R.A., and Tanaka, K. (2001). Human ocular dominance columns as revealed by high-field functional magnetic resonance imaging. *Neuron* 32, 359-374. doi: 10.1016/s0896-6273(01)00477-9.

Clare, S., and Jezzard, P. (2001). Rapid T(1) mapping using multislice echo planar imaging. *Magn Reson Med* 45, 630-634.

De Martino, F., Zimmermann, J., Muckli, L., Ugurbil, K., Yacoub, E., and Goebel, R. (2013). Cortical depth dependent functional responses in humans at 7T: improved specificity with 3D GRASE. *PLoS One* 8, e60514. doi: 10.1371/journal.pone.0060514.

Deichmann, R., Good, C.D., Josephs, O., Ashburner, J., and Turner, R. (2000). Optimization of 3-D MP-RAGE sequences for structural brain imaging. *Neuroimage* 12, 112-127. doi: 10.1006/nimg.2000.0601.

Duvernoy, H.M., Delon, S., and Vannson, J. (1981). Cortical blood vessels of the human brain. *Brain research bulletin* 7, 519-579.

Ehses, P., Budde, J., Shajan, G., and Scheffler, K. (2013). T2-weighted BOLD fMRI at 9.4 T using a S2-SSFP-EPI sequence. *21st Annual Meeting of ISMRM* 21, 0414.

Eichfelder, G., and Gebhardt, M. (2011). Local specific absorption rate control for parallel transmission by virtual observation points. *Magnetic Resonance in Medicine* 66, 1468-1476.

Freeman, J., Brouwer, G.J., Heeger, D.J., and Merriam, E.P. (2011). Orientation decoding depends on maps, not columns. *J Neurosci* 31, 4792-4804. doi: 10.1523/JNEUROSCI.5160-10.2011.

Gardner, J.L. (2010). Is cortical vasculature functionally organized? *Neuroimage* 49**,** 1953-1956. doi: 10.1016/j.neuroimage.2009.07.004.

Goa, P.E., Koopmans, P.J., Poser, B.A., Barth, M., and Norris, D.G. (2014). BOLD fMRI signal characteristics of S1- and S2-SSFP at 7 Tesla. *Frontiers in Neuroscience* 8. doi: 10.3389/fnins.2014.00049.

Goa, P.E., Poser, B.A., and Barth, M. (2013). Modeling and suppression of respiration induced B0-fluctuations in non-balanced steady-state free precession sequences at 7 Tesla. *Magnetic Resonance Materials in Physics Biology and Medicine* 26**,** 377-387. doi: 10.1007/s10334-012-0343-6.

Goncalves, N.R., Ban, H., Sanchez-Panchuelo, R.M., Francis, S.T., Schluppeck, D., and Welchman, A.E. (2015). 7 tesla FMRI reveals systematic functional organization for binocular disparity in dorsal visual cortex. *J Neurosci* 35**,** 3056-3072. doi: 10.1523/jneurosci.3047-14.2015.

Harmer, J., Sanchez-Panchuelo, R.M., Bowtell, R., and Francis, S.T. (2012). Spatial location and strength of BOLD activation in high-spatial-resolution fMRI of the motor cortex: a comparison of spin echo and gradient echo fMRI at 7 T. *NMR Biomed* 25**,** 717-725. doi: 10.1002/nbm.1783.

Harrison, R.V., Harel, N., Panesar, J., and Mount, R.J. (2002). Blood capillary distribution correlates with hemodynamic-based functional imaging in cerebral cortex. *Cerebral Cortex* 12**,** 225-233.

Haxby, J.V., Gobbini, M.I., Furey, M.L., Ishai, A., Schouten, J.L., and Pietrini, P. (2001). Distributed and overlapping representations of faces and objects in ventral temporal cortex. *Science* 293**,** 2425-2430.

Hua, J., Qin, Q., Van Zijl, P.C., Pekar, J.J., and Jones, C.K. (2013b). Whole-brain three-dimensional T2-weighted BOLD functional magnetic resonance imaging at 7 Tesla. *Magn Reson Med*. doi: 10.1002/mrm.25055.

Kamitani, Y., and Tong, F. (2005). Decoding the visual and subjective contents of the human brain. *Nat Neurosci* 8**,** 679-685. doi: 10.1038/nn1444.

Katscher, U., Bornert, P., Leussler, C., and Van Den Brink, J.S. (2003). Transmit SENSE. *Magn Reson Med* 49**,** 144-150. doi: 10.1002/mrm.10353.

Koopmans, P.J., Barth, M., and Norris, D.G. (2010). Layer-Specific BOLD Activation in Human VI. *Human Brain Mapping* 31**,** 1297-1304. doi: 10.1002/hbm.20936.

Lustig, M., Donoho, D., and Pauly, J.M. (2007). Sparse MRI: The application of compressed sensing for rapid MR imaging. *Magn Reson Med* 58**,** 1182-1195. doi: 10.1002/mrm.21391.

Ma, D., Gulani, V., Seiberlich, N., Liu, K., Sunshine, J.L., Duerk, J.L., and Griswold, M.A. (2013). Magnetic resonance fingerprinting. *Nature* 495**,** 187-192. doi: 10.1038/nature11971.

Menon, R.S., Ogawa, S., Strupp, J.P., and Ugurbil, K. (1997). Ocular dominance in human V1 demonstrated by functional magnetic resonance imaging. *Journal of Neurophysiology* 77**,** 2780-2787.

Muckli, L., De Martino, F., Vizioli, L., Petro, L.S., Smith, F.W., Ugurbil, K., Goebel, R., and Yacoub, E. (2015). Contextual Feedback to Superficial Layers of V1. *Current Biology*.

Mugler, J.P., 3rd, Epstein, F.H., and Brookeman, J.R. (1992). Shaping the signal response during the approach to steady state in three-dimensional magnetization-prepared rapid gradient-echo imaging using variable flip angles. *Magn Reson Med* 28**,** 165-185. doi: 10.1002/mrm.1910280202.

Olman, C.A., Inati, S., and Heeger, D.J. (2007). The effect of large veins on spatial localization with GE BOLD at 3 T: Displacement, not blurring. *Neuroimage* 34**,** 1126-1135.

Panchuelo, R.M.S., Schluppeck, D., Harmer, J., Bowtell, R., and Francis, S. (2015). Assessing the Spatial Precision of SE and GE-BOLD Contrast at 7 Tesla. *Brain topography* 28**,** 62-65.

Polimeni, J.R., Bianciardi, M., Keil, B., and Wald, L.L. (2015). Cortical depth dependence of physiological fluctuations and whole-brain resting-state functional connectivity at 7T. *23nd Annual Meeting of ISMRM* 23**,** 592.

Polimeni, J.R., Fischl, B., Greve, D.N., and Wald, L.L. (2010). Laminar analysis of 7T BOLD using an imposed spatial activation pattern in human V1. *Neuroimage* 52**,** 1334-1346. doi: 10.1016/j.neuroimage.2010.05.005.

Poser, B.A., Anderson, R.J., Guérin, B., Setsompop, K., Deng, W., Mareyam, A., Serano, P., Wald, L.L., and Stenger, V.A. (2014). Simultaneous multislice excitation by parallel transmission. *Magnetic Resonance in Medicine* 71**,** 1416-1427.

Renvall, V., Witzel, T., Wald, L.L., and Polimeni, J.R. (2014). Fast variable inversion-recovery time EPI for anatomical reference and quantitative T1 mapping. *22nd Annual Meeting of ISMRM* 22**,** 4282.

Scheffler, K., and Ehses, P. (2015). High-resolution mapping of neuronal activation with balanced SSFP at 9.4 tesla. *Magnetic resonance in medicine*.

Setsompop, K., Kimmlingen, R., Eberlein, E., Witzel, T., Cohen-Adad, J., Mcnab, J.A., Keil, B., Tisdall, M.D., Hoecht, P., and Dietz, P. (2013). Pushing the limits of in vivo diffusion MRI for the Human Connectome Project. *Neuroimage* 80**,** 220-233.

Shmuel, A., Chaimow, D., Raddatz, G., Ugurbil, K., and Yacoub, E. (2010). Mechanisms underlying decoding at 7 T: ocular dominance columns, broad structures, and macroscopic blood vessels in V1 convey information on the stimulated eye. *Neuroimage* 49**,** 1957-1964. doi: 10.1016/j.neuroimage.2009.08.040.

Shrivastava, D., Hanson, T., Schlentz, R., Gallaghar, W., Snyder, C., Delabarre, L., Prakash, S., Iaizzo, P., and Vaughan, J.T. (2008). Radiofrequency heating at 9.4T: in vivo temperature measurement results in swine. *Magn Reson Med* 59**,** 73-78. doi: 10.1002/mrm.21425.

Smith, F.W., and Muckli, L. (2010). Nonstimulated early visual areas carry information about surrounding context. *Proc Natl Acad Sci U S A* 107**,** 20099-20103. doi: 10.1073/pnas.1000233107.

Stöcker, T., and Shah, N.J. (2006). MP-SAGE: A new MP-RAGE sequence with enhanced SNR and CNR for brain imaging utilizing square-spiral phase encoding and variable flip angles. *Magnetic resonance in medicine* 56**,** 824-834.

Triantafyllou, C., Polimeni, J.R., Elschot, M., and Wald, L.L. (2009). Physiological Noise in Gradient Echo and Spin Echo EPI at 3T and 7T. *17th Annual Meeting International Society for Magnetic Resonance in Medicine***,** 122.

Ugurbil, K., Xu, J., Auerbach, E.J., Moeller, S., Vu, A.T., Duarte-Carvajalino, J.M., Lenglet, C., Wu, X., Schmitter, S., Van De Moortele, P.F., Strupp, J., Sapiro, G., De Martino, F., Wang, D., Harel, N., Garwood, M., Chen, L., Feinberg, D.A., Smith, S.M., Miller, K.L., Sotiropoulos, S.N., Jbabdi, S., Andersson, J.L., Behrens, T.E., Glasser, M.F., Van Essen, D.C., and Yacoub, E. (2013). Pushing spatial and temporal resolution for functional and diffusion MRI in the Human Connectome Project. *Neuroimage* 80**,** 80-104. doi: 10.1016/j.neuroimage.2013.05.012.

Uludag, K., Dubowitz, D.J., and Buxton, R.B. (2005). "Principles of functional imaging of the brain.," in *Clinical Magnetic Resonance Imaging (3rd Ed),* eds. R.R. Edelmann, J.R. Hesselink & M.B. Zlatkin. (England).

Uludag, K., Muller-Bierl, B., and Ugurbil, K. (2009). An integrative model for neuronal activity-induced signal changes for gradient and spin echo functional imaging. *Neuroimage* 48**,** 150-165. doi: 10.1016/j.neuroimage.2009.05.051.

Van Der Kouwe, A.J., Tisdall, M.D., Bhat, H., Fischl, B., and Polimeni, J.R. (2014). Multiple Echo and Inversion Time MPRAGE with Inner Loop GRAPPA Acceleration and Prospective Motion Correction for Minimally Distorted Multispectral Brain Morphometry. *22nd Annual Meeting of ISMRM* 22**,** 120.

Winawer, J., Horiguchi, H., Sayres, R.A., Amano, K., and Wandell, B.A. (2010). Mapping hV4 and ventral occipital cortex: the venous eclipse. *Journal of Vision* 10**,** 1.

Wu, X., Schmitter, S., Auerbach, E.J., Moeller, S., Uğurbil, K., and De Moortele, V. (2013). Simultaneous multislice multiband parallel radiofrequency excitation with independent slice-specific transmit B1 homogenization. *Magnetic Resonance in Medicine* 70**,** 630-638.

Xu, J., Moeller, S., Auerbach, E.J., Strupp, J., Smith, S.M., Feinberg, D.A., Yacoub, E., and Ugurbil, K. (2013). Evaluation of slice accelerations using multiband echo planar imaging at 3 T. *Neuroimage* 83**,** 991-1001. doi: 10.1016/j.neuroimage.2013.07.055.

Yacoub, E., Harel, N., and Ugurbil, K. (2008). High-field fMRI unveils orientation columns in humans. *Proc Natl Acad Sci U S A* 105**,** 10607-10612. doi: 10.1073/pnas.0804110105.

Yacoub, E., Shmuel, A., Logothetis, N., and Ugurbil, K. (2007). Robust detection of ocular dominance columns in humans using Hahn Spin Echo BOLD functional MRI at 7 Tesla. *Neuroimage* 37**,** 1161-1177. doi: 10.1016/j.neuroimage.2007.05.020.

Yacoub, E., Van De Moortele, P.F., Shmuel, A., and Ugurbil, K. (2005). Signal and noise characteristics of Hahn SE and GE BOLD fMRI at 7 T in humans. *Neuroimage* 24**,** 738-750. doi: 10.1016/j.neuroimage.2004.09.002.

Zhu, Y. (2004). Parallel excitation with an array of transmit coils. *Magnetic Resonance in Medicine* 51**,** 775-784.

Zimmermann, J., Goebel, R., De Martino, F., Van De Moortele, P.F., Feinberg, D., Adriany, G., Chaimow, D., Shmuel, A., Ugurbil, K., and Yacoub, E. (2011). Mapping the organization of axis of motion selective features in human area MT using high-field fMRI. *PLoS One* 6**,** e28716. doi: 10.1371/journal.pone.0028716.